



1 **Measurement report: Characteristics of**
2 **nitrogen-containing organics in PM_{2.5} in Urumqi,**
3 **northwest China: differential impacts of**
4 **combustion of fresh and old-age biomass**
5 **materials**

6

7 Yi-Jia Ma¹, Yu Xu^{2,*}, Ting Yang¹, Hong-Wei Xiao², Hua-Yun Xiao²

8

9 ¹School of Environmental Science and Engineering, Shanghai Jiao Tong University,

10 Shanghai 200240, China

11 ²School of Agriculture and Biology, Shanghai Jiao Tong University, Shanghai 200240,

12 China

13

14

15

16

17

18

*Corresponding authors

19

Yu Xu

20

E-mail: xuyu360@sjtu.edu.cn

21

22

23

24



25 **Abstract:** Nitrogen-containing organic compounds (NOCs) are abundant and
26 important aerosol components, deeply involving in global nitrogen cycle. However, the
27 sources and formation processes of NOCs remain largely unknown, particularly in the
28 city (Urumqi, China) farthest from the ocean worldwide. Here, NOCs in PM_{2.5} collected
29 in Urumqi over a one-year period were characterized by ultrahigh-resolution mass
30 spectrometry. The abundance of CHON compounds (mainly poor-O unsaturated
31 aliphatic-like species) in the positive ion mode was higher in the warm period than in
32 the cold period, which was largely attributed to the contribution of fresh biomass
33 material combustion (e.g., forest fires) associated with amidation of unsaturated fatty
34 acids in the warm period, rather than the oxidation processes. However, CHON
35 compounds (mainly nitro-aromatic species) in the negative ion mode increased
36 significantly in the cold period, which was tightly related to old-age biomass
37 combustion (e.g., dry straws) in wintertime Urumqi. For CHN compounds, we found
38 that alkyl nitriles and aromatic CNH compounds showed higher abundance in the warm
39 and cold periods, respectively. It further confirmed different impacts of the combustion
40 of fresh- and old-age biomass materials on NOC compositions. Our results clarify the
41 mechanisms by which fresh and old-age biomass materials emitted different NOCs.

42

43 **Keywords:** Aerosols, Organic nitrogen, Molecular composition, Fresh biomass, Old-
44 age biomass

45

46



47 **1. Introduction**

48 Fine particulate matter (PM_{2.5}) is a typical atmospheric pollutant, which can affect
49 the global climate system, as well as urban air quality and human health (Seinfeld et al.,
50 2016; Wang et al., 2021a). Organic aerosol (OA) contributes significantly (20–90%) to
51 PM_{2.5} mass concentration in most polluted areas worldwide (Zhang et al., 2007; Han et
52 al., 2023). However, up to 77% of molecules in OA include nitrogen-containing
53 functional groups (Ditto et al., 2020; Kenagy et al., 2021), which has been suggested to
54 play important roles in the formation, transformation, acidity, and hygroscopicity of OA
55 (Xu et al., 2020; Wang et al., 2017b; Laskin et al., 2009). Moreover, the modified forms
56 of some nitrogen-containing organic compounds (NOCs) and volatile organic
57 compounds (VOCs) by ozone (O₃), hydroxyl radical (•OH), and nitrogen oxide (NO_x)
58 can lead to an increase in the health hazards of OA, among which nitrated amino acids
59 and nitrated polycyclic aromatic hydrocarbons are two representative hazards (Franze
60 et al., 2005; Bandowe and Meusel, 2017). Thus, the identification of aerosol NOCs at
61 the molecular level is important for improving our understanding of the precursors,
62 sources, and formation processes of nitrogen-containing OA.

63 Previous observations in urban, rural, marine, and forest areas have suggested that
64 the molecular composition and relative abundance of aerosol NOCs were spatially
65 different (Samy and Hays, 2013; Jiang et al., 2022; Lin et al., 2012; Xu et al., 2023).
66 These differences can be mainly attributed to the diverse sources and formation
67 mechanisms of aerosol NOCs. Commonly reported primary sources include
68 combustion process releases and natural emissions (e.g., soils, plant debris, pollen, and



69 ocean) (Song et al., 2022; Wang et al., 2017b; Cape et al., 2011; Lin et al., 2023). In
70 addition, aerosol NOCs can also be tightly associated with secondary formation
71 processes involving the reactions of reactive nitrogen with VOCs or particle-phase
72 CHO compounds (Bandowe and Meusel, 2017; Zarzana et al., 2012; Laskin et al.,
73 2014). For example, laboratory experiments have suggested that the oxidation of
74 isoprene and α - β -pinene in the presence of NO_x can result in the formation of organic
75 nitrates (e.g., methacryloyl peroxyxynitrate, dihydroxynitrates, and monohydroxynitrates)
76 (Surratt et al., 2010; Rollins et al., 2012; Nguyen et al., 2015). The reduced nitrogen
77 species (e.g., NH_3 , NH_4^+ , and organic amines) have been demonstrated to contribute to
78 the formation of NOCs through "carbonyl-to-imine" transformations in the laboratory
79 experiments (Zarzana et al., 2012; Laskin et al., 2014). In the field observation studies,
80 NOCs in particulate matter were analyzed at the molecular level to indicate on their
81 sources and formation mechanisms (Jiang et al., 2022; Lin et al., 2012; Zhong et al.,
82 2023). Xu et al. (2023) characterized the variations of molecular compositions in urban
83 road $\text{PM}_{2.5}$, suggesting that organic nitrates increased largely through the interactions
84 of atmospheric oxidants, reactive gas-phase organics, and aerosol liquid water. Several
85 field studies conducted in Beijing (China) and Guangzhou (China) also suggested that
86 the molecular compositions and formation of NOCs were tightly associated with the
87 environmental conditions (Jiang et al., 2022; Lin et al., 2012; Xie et al., 2020).
88 Generally, most of studies on aerosol NOCs were performed in economically developed
89 regions, as well as in forest and marine areas (Jiang et al., 2022; Wang et al., 2017a;
90 Ditto et al., 2022b; Altieri et al., 2016; Miyazaki et al., 2014). In contrast, few studies



91 have investigated the sources and atmospheric transformation of NOCs in the northwest
92 border urban of China (e.g., Urumqi) with fragile ecology and harsh environmental
93 conditions (e.g., cold winter and dry summer), which may hinder our comprehensive
94 and in-depth understanding of the formation process of NOCs in ambient aerosols.

95 Biomass burning emissions were widely reported in the source identification of
96 aerosol NOCs in northern and southwestern China because of heating and cooking
97 needs (Zhong et al., 2023; Wang et al., 2021c; Chen et al., 2017). A recent observation
98 study in urban Tianjin suggested that most CHON compounds in wintertime PM_{2.5}
99 originated from biomass burning (Zhong et al., 2023). The CHN₂ compounds have been
100 identified in biomass burning OA (BBOA) (Laskin et al., 2009; Wang et al., 2017b).
101 Moreover, the high temperature generated by biomass burning can facilitate the release
102 of ammonia, a process which caused the reaction of carboxylic acids (e.g., oleic acid)
103 with ammonia to form amides and alkyl nitriles (Radzi Bin Abas et al., 2004; Simoneit
104 et al., 2003). Interestingly, we found that biomass burning in rural China typically
105 includes both fresh biomass materials (e.g., forest fires) and old-age biomass materials
106 (e.g., straw after autumn harvest, fallen leaf, and deadwood). Fresh biomass is rich in
107 oils and proteins, whereas old-age biomass materials are usually oligotrophic due to the
108 transfer of nutrients to tender tissues or fruits (Jian et al., 2016; Xu and Xiao, 2017).
109 Thus, NOCs released from different types of biomass combustion may vary in
110 molecular compositions. However, there are large gaps in our current knowledge about
111 the impacts of fresh and old-age biomass burning on NOCs in ambient aerosols.

112 Urumqi (northwest China) is the largest inland city farthest from the ocean in the



113 world, which is becoming increasingly prominent due to the national strategy of the
114 "One Belt, One Road". The city and neighboring countries have a dry summer that can
115 easily trigger forest fires (Bátori et al., 2018; Xu et al., 2021), while the winter is very
116 cold with intensive old-age biomass and fuel combustion for heating (Ren et al., 2017).
117 In this study, we presented one-year ambient measurements of the chemical
118 compositions in PM_{2.5} collected from Urumqi. The specific aims of this study are (1) to
119 investigate the molecular-level speciation of functionalized organic nitrogen
120 compounds via a high-resolution mass spectrometry with positive (ESI+) and negative
121 (ESI-) ionizations and (2) to investigate the potential sources and formation processes
122 for NOCs with a special focus on the relative influences of fresh and old-age biomass
123 burning.

124

125 **2. Materials and methods**

126 **2.1. Study site description and sample collection**

127 The study was conducted in Urumqi city with an average altitude of 800 m. The
128 region has an arid temperate continental climate with an annual mean temperature of
129 7.4 ± 13.9 °C and an annual mean rainfall of 27.8 mm. The sampling site is located in
130 the suburban area (Boda campus of Xinjiang University) of the city (87.75°E, 43.86°N)
131 (**Figure S1**), which is characterized by low population and traffic density. This is
132 because Urumqi is relatively vast and sparsely populated compared to developed
133 coastal cities in China (Qizhi et al., 2016). Additionally, the area is surrounded by
134 mountains on three sides, resulting in the difficulty in diffusion of air pollutants. The



135 dominant forest trees in this area are *Picea schrenkiana*, *Betula tianschanica* Rupr.,
136 *Populus talassica* Kom., and *Ulmus pumila* L.. The dry climate and strong sunlight in
137 the warm period ($18.81 \pm 6.4^\circ\text{C}$, **Table S1**) would be the main culprits of forest fires in
138 the local and nearby areas. In the cold period ($-1.96 \pm 11.26^\circ\text{C}$) (**Table S1**), the
139 centralized heating and old-age biomass burning may be the main contributors of local
140 air pollution. Thus, it provides an unexpected opportunity to investigate the potentially
141 differential impacts of fresh and old-age biomass burning on aerosol NOCs.

142 A high-volume air sampler (Series 2031, Laoying, China) was set up on the
143 rooftop of a building (School of Geology and Mining Engineering, Xinjiang University).
144 PM_{2.5} samples ($n = 73$) were collected every 5 days with a duration of ~ 24 h onto
145 prebaked (450°C for ~ 10 h) quartz fiber filters (Pallflex, Pall Corporation, USA) from
146 1 March 2018 to 26 February 2019. One blank filter was collected every month ($n =$
147 12). All filter samples were stored at -30°C until further analysis. The meteorological
148 data (e.g., temperature and relative humidity) and the concentrations of O₃ and NO_x
149 were daily recorded from the adjacent environmental monitoring station during the
150 sampling campaigns. In addition, the trajectories (72 h) of air masses arriving at the
151 sampling site at each sampling event were calculated to investigate the potential
152 influence of pollutant transport on aerosol NOCs.

153

154 **2.2. Chemical analysis**

155 A portion of each filter sample was extracted twice using methanol (LC-MS grade,
156 CNW Technologies Ltd.) under sonication in a chilled ice slurry ($\sim 4^\circ\text{C}$). The extracted



157 solutions were filtered through a polytetrafluoroethylene syringe filter (0.22 μm , CNW
158 Technologies GmbH). Subsequently, the extracts were concentrated to 300 μL with a
159 gentle stream of gaseous nitrogen (Shanghai Likang Gas Co., Ltd). The final extracts
160 were divided into two parts, which were analyzed separately as described in previous
161 study (Wang et al., 2021b) under ESI⁺ and ESI⁻ modes using an UPLC-ESI-QToFMS
162 (Xevo G2-XS QToFMS, Waters) system. It should be pointed out that UPLC-ESI-MS
163 (i.e., TOF-only) was used to identify molecular formulas of organic matter, while the
164 functional groups of the target molecule formulas were deciphered by UPLC-ESI-
165 MS/MS (i.e., tandem mass spectrometry). Ions obtained from m/z 50–700 were
166 assigned molecule formulas via assuming hydrogen or sodium adducts in ESI⁺ mode
167 and deprotonation in ESI⁻ mode. Detailed chromatographic conditions, parameter
168 selection, and quality control were displayed in the Supplement (**Sect. S1**). Notably,
169 there may be differences in ionization efficiencies between compound types. However,
170 the exact impacts of ionization efficiency on multifunctional compounds in a complex
171 mixture are uncertain and difficult to evaluate (Ditto et al., 2022b; Yang et al., 2023).
172 Thus, the intercomparison across compound relative abundance without considering
173 potentially differentiated ionization efficiency was conducted in this study, which was
174 similar to many previous studies (Xu et al., 2023; Jiang et al., 2022).

175 For the measurement of inorganic ions, a portion of each filter sample was
176 ultrasonically extracted with Milli-Q water (18 M Ω cm) in an ice-water bath (\sim 4 °C).
177 The extract solutions were then filtered via a polytetrafluoroethylene syringe filter (0.22
178 μm , Millipore, Billerica, MA). The concentrations of water-soluble inorganic ions



179 including NO_3^- , SO_4^{2-} , Cl^- , Ca^{2+} , Mg^{2+} , Na^+ , and NH_4^+ in the samples were determined
180 using an ion chromatograph system (Dionex Aquion, Thermo Scientific, USA) (Xu et
181 al., 2022a; Lin et al., 2023).

182

183 **2.3. Compound categorization and predictions of ALW, pH, and hydroxyl radical.**

184 The molecular formulas identified by UPLC-ESI-QToFMS were classified into
185 several major compound classes based on their elemental compositions (i.e., C, H, O,
186 and N), primarily including CHO, CHON, and CHN groups in the ESI+ mode and CHO
187 and CHON groups in the ESI- mode (Wang et al., 2017b). All of the detected molecules
188 were reported as neutral molecules, unless stated otherwise. The double-bond
189 equivalent (DBE) and carbon oxidation state (OS_C) were calculated to reflect the
190 unsaturation degree of the organics and the composition evolution of organics that
191 underwent oxidation processes, respectively (details in **Sect. S2**) (Kroll et al., 2011; Xu
192 et al., 2023). Additionally, the modified aromaticity index (AI_{mod}) was also calculated
193 to indicate the aromaticity of organic compounds (details in **Sect. S2**) (Koch and
194 Dittmar, 2006).

195 A thermodynamic model (ISORROPIA-II) was applied to predict the mass
196 concentration of aerosol liquid water (ALW) and the value of pH with particle-phase
197 ion concentrations as well as ambient temperature and relative humidity as the inputs,
198 as detailed in our previous publications (Xu et al., 2020; Xu et al., 2023; Xu et al.,
199 2022b). The concentrations of ambient $\bullet\text{OH}$ were predicted using empirical formula
200 (Ehhalt and Rohrer, 2000; Wang et al., 2020).



201

202 **3. Results and discussion**

203 **3.1. Overall molecular characterization of organic aerosols**

204 **Figures 1a** and **1c** show the mass spectra of organic compounds detected in ESI+
205 and ESI-, respectively. More compounds were identified in ESI+ (1885 molecular
206 formulas) than in ESI- (438 molecular formulas) (**Table S2**), which was similar to
207 previous reports about the molecular characteristic of biomass burning aerosols and
208 urban aerosols (Jiang et al., 2022; Wang et al., 2017b). The molecular weights of the
209 compounds with relatively high signal intensity mainly ranged from 100 Da to 500 Da
210 in ESI+, which was larger than those (100–300 Da) observed in the urban (Changchun,
211 Guangzhou, and Shanghai) (Wang et al., 2021a) and agriculture (Suixi) (Wang et al.,
212 2017b) regions of China. In contrast, the species with the strong signal intensity fell
213 between 100 Da and 300 Da in ESI-. This mass range detected in Urumqi organic
214 aerosols was comparable to previous observations in urban aerosols (Han et al., 2023)
215 but significantly lower than that in firework-related urban aerosols (300–400 Da) (Xie
216 et al., 2020). On average, the molecular number and relative abundance of CHON
217 compounds (150–500 Da) were dominant in ESI+, accounting for 45.99% of the total
218 molecular number and $62.70 \pm 6.83\%$ of the total signal intensity (**Figures 1a** and
219 **Table S2**). CHO compounds were the second most abundant categories ($28.76 \pm 4.75\%$
220 of the total signal intensity), followed by CHN compounds. However, previous
221 observations conducted in Shanghai, Guangzhou, and Changchun suggested that the
222 compounds in ESI+ were dominated by CHN and CHON species (Wang et al., 2021a).



223 In ESI⁻, although the number of CHON compounds was less than CHO, the relative
224 abundance of CHON compounds (150–250 Da) was higher (**Figures 1d** and **Table**
225 **S2**). The finding was consistent with the results obtained in Shanghai and Changchun
226 but different from the case in Guangzhou (Wang et al., 2021a). The average H/C ratios
227 of CHO (1.62–1.66) and CHON (1.79–1.83) compounds in ESI⁺ mode (**Table S3**)
228 were higher than those (0.94–1.13 and 1.27–1.47) in Changchun, Shanghai, and
229 Guangzhou (Wang et al., 2021a). However, the average O/C ratios of CHO (0.25–0.3)
230 and CHON (0.22–0.3) compounds in ESI⁺ mode (**Table S3**) were less than those
231 (0.42–0.43 and 0.27–0.45) in the urban areas (Shanghai and Guangzhou) (Wang et al.,
232 2021a). Overall, these dissimilarities in molecular characteristics of organic aerosols
233 between Urumqi and other areas may be attributed to their different sources and
234 formation mechanisms.

235 **Figures 1b** and **1d** show the time series of the fractional distributions of various
236 organic matter categories in different ion modes. The abundance of CHO compounds
237 in ESI⁺ exhibited a temporal variation similar to that of CHON compounds ($r = 0.51$,
238 $P < 0.01$), with increased levels in the warm period. This indicated that CHO
239 compounds may be important precursors for the formation of NOCs or that they have
240 similar origins. Previous simulation experiment has demonstrated that higher
241 temperatures can result in an increase in the concentration of the oxygenated organic
242 molecules, while lower temperatures can allow less oxidized species to condense
243 (Stolzenburg et al., 2018; Frege et al., 2018). In addition, solar radiation and
244 atmospheric oxidation capacity are also important factors promoting the formation of



245 more oxygenated organic molecules (Li et al., 2022; Liu et al., 2022). Air temperature,
246 radiation, and atmospheric oxidation capacity were much higher in the warm period
247 than in the cold period in Urumqi (**Table S1**) (Wan et al., 2021), which may be partly
248 responsible for increased abundances of CHO and CHON compounds in the warm
249 period. However, the abundance of CHN compounds tended to increase from the warm
250 period to the cold period. Since the ESI+ mode is highly sensitive to protonatable
251 species, organic amines were expected to predominate the CHN compounds (Han et al.,
252 2023; Wang et al., 2021a). It is well documented that the formation of amine salt in the
253 particle phase is tightly associated with aerosol acidity and water (Liu et al., 2023).
254 Thus, the reduced pH value and increased ALW level in the cold period (**Table S1**)
255 provided greater potential for converting gaseous amines into particles.

256 In ESI- mode, the abundances of CHON and CHO exhibited a significantly
257 increased level in the cold period (**Figure 1d**), a variation pattern which was completely
258 opposite to the case in ESI+ mode. The ESI- mode is more sensitive to deprotonatable
259 compounds, such as nitrophenols, organic nitrates, organosulfates, and organic acids
260 (Jiang et al., 2022; Lin et al., 2012). The formations of these compounds were highly
261 impacted by ALW and aerosol acidity (Ma et al., 2021; Smith et al., 2014; Zhou et al.,
262 2023; Xu et al., 2023). However, Urumqi has dry and dusty weather, particularly in
263 warm period, resulting in a quite low ALW concentration ($1.86 \pm 1.90 \mu\text{g m}^{-3}$) in the
264 warm period (**Table S1**). Moreover, the calculated mean pH values were 6 during the
265 warm period without considering the influence of gaseous ammonia (**Table S1**).
266 Previous studies have suggested that a bias correction of 1 unit should be considered



267 for the prediction of aerosol pH when lacking of ammonia measurements (Guo et al.,
268 2015; Wang et al., 2021c). This implied that the actual aerosol acidity in the warm
269 period in Urumqi should be neutral or slightly alkaline. Obviously, the aerosol
270 characteristics of the warm period in Urumqi may hinder the formation of these organic
271 compounds measured in ESI⁻ mode. In contrast, the increased ALW concentration and
272 decreased pH value during the cold period can facilitate the formation of CHO and
273 CHON compounds through the partitioning of gas-phase species to the particles and
274 subsequent aqueous phase reactions (Xu et al., 2020; Xu et al., 2023). Furthermore, the
275 total signal intensity of CHO compounds was significantly correlated with that of
276 CHON ($r = 0.62$, $P < 0.01$), indicating that they may have similar origins or that CHO
277 compounds may serve as important precursors for CHON compound formation. It
278 should be noted that this study mainly focuses on NOCs, therefore sulfur-containing
279 species were not discussed. In general, the differentiated seasonal variation patterns for
280 the different types of NOCs measured here can be attributed to the unique
281 meteorological conditions in Urumqi and different ionization mechanisms in ESI⁺ and
282 ESI⁻ modes. The sources and formation mechanisms of NOCs will be further discussed
283 in the following sections.

284

285 **3.2. Seasonally differential sources and formation mechanisms of CHON** 286 **compounds**

287 CHON compounds can be products of reactions between CHO species and
288 reactive nitrogen species (NO_x , NH_3 , and NH_4^+) (Lee et al., 2016; De Haan et al., 2017),



289 as also partly implied by significant positive correlations ($r = 0.51\text{--}0.62$, $P < 0.01$)
290 between total signal intensity of CHO and CHON compounds in both ESI+ and ESI-
291 modes. Thus, CHO compounds were further classified based on their OS_C values to
292 preliminarily explore their origins and linkages with CHON compound formation
293 (**Figures 2a** and **2b**). In ESI+ mode, the OS_C values of the detected CHO compounds
294 (-1.75 to 0.5) were higher than those of primary vehicle exhausts (-2.0 to -1.9) (Aiken
295 et al., 2008), likely indicating a weak (or indirect) contribution of primary vehicle
296 exhausts to CHO molecules in Urumqi. The signal intensity of BBOA dominated the
297 total OA signal intensity and was higher in the warm period than in the cold period
298 (**Figure 2e**). However, previous studies conducted in China (e.g., Beijing, Xi'an,
299 Shanghai, and Liaocheng) suggested that biomass burning was more significant in the
300 cold seasons (Li et al., 2023; Wang et al., 2017a; Chen et al., 2017; Wang et al., 2009;
301 Wang et al., 2018). Furthermore, we found that the oxygen-poor unsaturated aliphatic
302 compounds showed a high signal intensity in the warm period and that the signal
303 intensities of all categories of compounds in the warm period were weakly correlated
304 with atmospheric oxidants (i.e., O_3 and $\bullet OH$) ($r < 0.1$, $P > 0.05$). Thus, the formation or
305 source of CHO compounds in the warm period may not be mainly controlled by high
306 atmospheric oxidation, but rather by biomass burning, which was distinguished from
307 previous reports (Duan et al., 2020; Kondo et al., 2007). This consideration was also
308 supported by the fact that there were significantly more fire spots in the warm period
309 than in the cold period (**Figure 3**). It should be noted that the materials used for biomass
310 burning in the cold period in rural China are typically old-age plant tissues (**Figure S3**),



311 while biomass burning in the warm season is mainly attributed to forest fires or
312 wildfires (relatively fresh biomass). Accordingly, a large number of fresh biomass
313 material burning occurred from April to October each year in the neighboring countries
314 (e.g., Kazakhstan) (Xu et al., 2021) or regions of Urumqi (due to drought) (**Figure 3**)
315 may be largely responsible for high CHO compound abundance in the warm period.

316 The CHO species in ESI⁻ had higher OS_C (-1.85 to 1.1) than those in ESI⁺
317 (**Figures 2c and 2d**), which was consistent with a recent study conducted in Guangzhou,
318 China (Zou et al., 2023). The predominant subgroups of CHO in ESI⁻ were BBOA and
319 semivolatile oxidized OA (SV-OOA), which was different from the observation in
320 Shanghai (dominated by SV-OOA and low-volatility oxidized OA) (Wang et al., 2017a).
321 Additionally, some specific saturated and unsaturated aliphatic CHO substances (i.e.,
322 C₁₂₋₁₈H_nO₂) in ESI⁻ showed higher abundance in the warm season than in the cold
323 season, which was contrary to the variation pattern of other CHO compounds. These
324 C₁₂₋₁₈H_nO₂ compounds were found to be mainly fatty acids, such as stearic acid
325 (C₁₈H₃₆O₂), oleic acid (C₁₈H₃₄O₂), linoleic acid (C₁₈H₃₂O₂), palmitic acid
326 (C₁₆H₃₂O₂), and palmitoleic acid (C₁₆H₃₀O₂) (**Figure S4**), all of which usually
327 accumulate in plants, particularly *Suaeda aralocaspica* (W. Hogg and T. Gillan, 1984;
328 Wang et al., 2011). Interestingly, this plant was widely distributed in Central Asia as
329 well as in the southern edge of the Junggar Basin in Xinjiang, China (Wang et al., 2011).
330 Although fatty acids can also originate from food cooking (Zhao et al., 2007), there
331 seems to be no seasonal differences in cooking behavior locally. Thus, these results
332 further confirmed our consideration that the abundance of CHO compounds in the



333 warm period was highly impacted by fresh biomass material burning (e.g., forest fires
334 or wildfires).

335 CHON molecules in ESI⁺ were mainly identified as unsaturated aliphatic-like
336 compounds with poor oxygen (**Figures 4a** and **4b**), accounting for more than 70% of
337 the total signal intensities of CHON species (**Figure S5**). The signal intensity of CHON
338 species in ESI⁺ was greater in the warm period than in the cold period (**Figure 4e**).
339 Moreover, BBOA contributed to 56.9 % of the total CHON signal intensity in the warm
340 period (**Figure S6**). These characteristics of CHON compounds were similar to those
341 of CHO. Considering a significant positive correlation ($r = 0.62$, $P < 0.01$) between the
342 total signal intensity of CHO and CHON compounds in ESI⁺, we thus concluded that
343 primary sources (i.e., fresh biomass material burning) were also one of the main sources
344 of CHON compounds. In this study, CHON compounds with $O/N < 3$ contributed 76.48
345 $\pm 1.11\%$ of total CHON species in ESI⁺ (**Figure S7**), which was much larger than the
346 results observed in urban Tianjin in winter (less than 20%) (Zhong et al., 2023). In
347 particular, $C_{16}H_{33}ON$, $C_{18}H_{37}ON$, $C_{18}H_{35}ON$, $C_{18}H_{33}ON$, $C_{18}H_{31}ON$, and $C_{20}H_{33}ON$
348 showed a high abundance, together accounting for $55.04 \pm 7.09\%$ of the total CHON
349 abundance (**Table S4**). The carbon number of these compounds was consistent with
350 that of fatty acids mentioned above; moreover, their abundances showed a positive
351 correlation ($r = 0.43\text{--}0.81$, $P < 0.01$) with the abundances of corresponding fatty acids
352 in the warm period. In contrast, these CHON compounds only showed a weak
353 correlation ($r = -0.24 \sim 0.33$) with atmospheric oxidants (e.g., $\bullet OH$, O_3 , and NO_x). Thus,
354 the formation mechanism of biomass burning-related NOCs in Urumqi during the warm

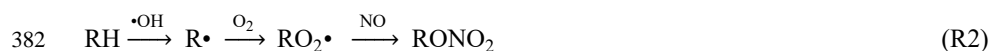


355 period may be the interaction between fatty acids and reduced nitrogen species (e.g.,
356 NH_3) rather than the oxidation pathway involving CHO compounds and NO_x .

357 A recent laboratory study has suggested that NH_3 produced during the thermal
358 degradation of amino acids can react with oleic acid from the pyrolysis of triglycerides
359 to form amides (R1) (Ditto et al., 2022a). As discussed above, the combustion of fresh
360 biomass materials (e.g., forest fires or wildfires) can release abundant fatty acids. In
361 addition, wildfires can also emit large amounts of NH_3 , with an average emission factor
362 more than twice NH_3 emission factor of agricultural fires (Tomsche et al., 2023).
363 According to MS/MS analysis (**Table S5**), potential fatty acid-derived NOCs were
364 indeed identified as amides. Thus, we proposed that the high temperature generated
365 during wildfires or forest fires provides suitable conditions for the reaction of
366 carboxylic acids and NH_3 to form amides. The specific process was presented in **Figure**
367 **5** (Pathway 1). It has been suggested that atmospheric oxidants can oxidize olefins (R2
368 and R3) to form hydroxyl nitrates and carbonyl nitrates (Perring et al., 2013). Therefore,
369 fatty acids (oleic acid as a representative) released from fresh biomass material burning
370 may also rely on oxidation pathways to form NOCs (**Figure 5**, Pathway 2). It is worth
371 noting that some products with double bonds after the amidation of unsaturated fatty
372 acids can continue to undergo the reactions of R2 and R3 in the atmosphere, resulting
373 in the formation of nitrooxy amides (**Figure 5**, Pathway 3). However, we found that the
374 abundance of oleic acid-derived amides via Pathway 1 in the warm period was more
375 than 100 times higher than that of NOCs with $-\text{ONH}_2$ (thus, the impact of ionization
376 efficiency is expected to be less than 100 times) from Pathways 3. In the cold period,



377 the abundance of fatty acids-derived amides decreased dramatically (**Figure 5** and
378 **Figure S8**). Thus, the overall results demonstrated that the combustion of fresh biomass
379 materials indeed contributed significantly to aerosol NOCs (e.g., amides) in the warm
380 period in Urumqi.



384 The CHON species detected in ESI⁻ were mainly aromatic-like compounds,
385 whose signal intensities were significantly greater in the cold period than in the warm
386 period (**Figures 4c,4e** and **Figure S5**). Moreover, we found that several nitro-aromatic
387 compounds, including C₆H₅O₃N, C₆H₅O₄N, C₇H₇O₃N, C₇H₇O₄N, C₇H₅O₅N, C₈H₉O₃N
388 (confirmed by their authentic standards in the LC/MS analysis), contributed up to 50%
389 of the total CHON (ESI⁻ mode) intensity (**Table S6**). Other NOCs with relatively high
390 signal intensity were mainly O₄₋₆N₂ species (contributed up to 25%), such as C₆H₄O₅N₂,
391 C₇H₄O₇N₂, C₇H₆O₅N₂, and C₇H₆O₆N₂, which have been suggested to be associated with
392 secondary photochemical or multiphase chemical processes (Harrison et al., 2005;
393 Cecinato et al., 2005; Salvador et al., 2021). However, the abovementioned nitro-
394 aromatic compounds including C₆H₅O₃N (nitrophenol), C₆H₅O₄N (nitrocatechol),
395 C₇H₇O₃N (methyl-nitrophenol), C₇H₇O₄N (methyl-nitrocatechol) were primarily
396 identified as tracers of straw and wood burning (old-age biomass materials commonly
397 used in suburban and rural China) (Iinuma et al., 2010; Kourtchev et al., 2016). A study



398 about molecular characterization (ESI⁻ mode) of water-soluble aerosols emitted from
399 the combustion of old-age biomass materials (i.e., dry corn straw, rice straw, and pine
400 branches) and coal showed that OA from old-age biomass burning typically contained
401 much more nitro compounds and/or organonitrates than that from coal, while OA from
402 coal-smoke contained more sulfur-containing compounds (Song et al., 2018). Thus, the
403 old-age biomass burning associated with winter heating rather than coal combustion
404 may contribute a significant amount of aerosol NOCs (e.g., nitrophenols) in wintertime
405 Urumqi. However, it does not necessarily suggest that the importance of multiphase
406 chemistry in the formation of NOCs was ignorable, as indicated by relatively high
407 signal intensity of O_{4,6}N₂ species. In general, the differential molecular characteristics
408 of CHON species in different seasons in Urumqi can largely attributed to different
409 impacts of the combustion of fresh- and old-age biomass materials.

410

411 **3.3. CHN Molecule Evidence of Fresh and Old-age Biomass Burning in Different** 412 **Periods.**

413 **Figures 6a** and **6b** present the van Krevelen diagram of CHN compounds in the
414 cold and warm periods. The CHN₁ compounds with relatively high signal intensity
415 mainly contained 7–20 carbon atoms, among which C₅H₅N(CH₂)_n, C₉H₇N(CH₂)_n, and
416 C₁₃H₉N(CH₂)_n were dominant (78.68 ± 7.59 % of the total signal intensity of CHN₁
417 compounds in the cold period, **Table S7**). C₅H₅N(CH₂)_n could be identified as pyridine
418 and its homologues, which have been detected in freshly discharged BBOA (Dou et al.,
419 2015). Additionally, the abundance of C₅H₅N(CH₂)_n was positively correlated with that



420 of $C_9H_7N(CH_2)_n$, $C_{13}H_9N(CH_2)_n$, and nitro-aromatic compounds mentioned above ($r =$
421 $0.46\text{--}0.81$, $P < 0.01$), particularly in the cold period with old-age biomass burning for
422 heating. We further found that both the total signal intensity and aromaticity of CHN_1
423 species was much higher in the cold period (AI_{mod} of 0.52) than in the warm period
424 (AI_{mod} of 0.35) (**Figure 6** and **Figure S9**). It has been suggested that old-age leaves
425 contain more aromatic compounds compared to fresh leaves (Jian et al., 2016). Thus,
426 the overall results implied that old-age biomass burning had an important contribution
427 to the variation of CHN_1 compounds. In particular, the intensity of CHN_1 compounds
428 was significantly negatively correlated with the concentration of O_3 and $\cdot OH$ ($r = -0.44$
429 ~ -0.53 , $P < 0.01$), suggesting that atmospheric oxidation processes were the potential
430 pathway for amine removal rather than the sources of particle amine salts (Zahardis et
431 al., 2008; Qiu and Zhang, 2013). This result was different from the previous case
432 showing the formation processes of CHN_1 and its homologs in Guangzhou (South China)
433 were tightly related to photo-oxidation processes (Jiang et al., 2022). The CHN_2 species
434 showed a similar temporal variation pattern to the CHN_1 species. Moreover, the
435 abundances of total CHN_2 and major components ($C_{8-11}H_8N_2(CH_2)_n$, $C_{10}H_{14}N_2(CH_2)_n$,
436 $C_{10}H_{16}N_2(CH_2)_n$ and $C_5H_8N_2(CH_2)_n$) were positively correlated with that of total CHN_1
437 ($r = 0.55\text{--}0.90$, $P < 0.01$), but negatively correlated with the concentration of O_3
438 and $\cdot OH$ ($r = -0.43 \sim -0.60$, $P < 0.01$). Clearly, old-age biomass burning, particularly
439 in the cold period, also exerted significant impacts on the abundance of CHN_2
440 compounds, which was also supported by several previous studies (Laskin et al., 2009;
441 Wang et al., 2017b; Song et al., 2022).



442 Interestingly, we found some CHN species with 16–20 carbon atoms showed
443 higher abundance in the warm period than in the cold period, a pattern of which was
444 opposite to that of all other CNH compounds (**Figure 6c**). These $C_{16-20}N_1H_x$
445 compounds were further identified as alkyl nitriles (**Table S5**) (Simoneit et al., 2003).
446 In addition, the carbon number of the identified alkyl nitriles was consistent with those
447 of amides previously proposed to be produced by fresh biomass burning. Thus, we
448 proposed that fresh biomass material burning in the warm period may provide a
449 continuous high-temperature environment to promote the dehydration of amides
450 (**Figure 5**, Pathway 4). These alkyl nitriles with double bonds can continue to undergo
451 the reactions of R2 and R3 (**Figure 5**, Pathway 5). However, the signal intensity of the
452 nitrooxy products in the warm period was insignificantly correlated with the
453 concentration of O_3 , $\cdot OH$, and NO_x ($P > 0.05$), likely indicating a weak influence of
454 atmospheric oxidation on alkyl nitrile removal in this site. The high-temperature
455 dehydration of amides (e.g., erucamide) to form alkyl nitriles (e.g., erucyl nitrile) has
456 been demonstrated by Simoneit et al. (Simoneit et al., 2003) in a laboratory simulation
457 experiment. A study on BBOA also showed that alkyl nitriles can be serve as indicators
458 of biomass burning in the ambient atmosphere (Radzi Bin Abas et al., 2004).
459 Furthermore, the abundance of identified alkyl nitriles initially increased from March
460 and peaked in September and October (**Figure S10**), a pattern of which was consistent
461 with the interannual variation in wildfire areas (more in the warm period) in Central
462 Asian countries (Xu et al., 2021). Although cooking is also a potential source of alkyl
463 nitriles (Schauer et al., 1999), this activity does not have seasonal differences. In



464 contrast, the dramatically increased abundance of aromatic CNH compounds in the cold
465 period (**Figure S9**) can be attributed to the aqueous reactions of amines emitted from
466 old-age biomass material and coal combustion with acidic substances, as indicated by
467 significant correlations ($r = 0.61-0.95$, $P < 0.01$) between total CHN abundance and
468 SO_4^{2-} and NO_3^- concentrations. These findings further confirmed that the NOCs from
469 the combustion of fresh biomass materials in the warm period in suburban Urumqi were
470 compositionally different from those from old-age biomass burning in the cold period.

471

472 **4 Conclusions**

473 The complexity of NOCs restricts our understanding of its sources and formation
474 processes. In this study, the molecular compositions of organic aerosols in $\text{PM}_{2.5}$
475 collected in Urumqi over a one-year period were systematically characterized in both
476 ESI⁻ and ESI⁺ modes, with a major focus on NOCs. A large amount of NOCs were
477 identified, showing that NOCs in relatively highly oxidative and reduced forms can be
478 roughly distinguished via these two ionization modes. Based on the identification of
479 molecular markers of amides and alkyl nitriles (much higher in the warm period) and
480 the analysis of their formation mechanisms (less contribution of atmospheric oxidation),
481 we highlighted the important contribution of combustion of fresh biomass materials
482 such as forest fires and wildfires to NOCs in the warm season in Urumqi. In contrast,
483 the dramatically increased abundances of aromatic CNH compounds and nitro-aromatic
484 CHON compounds (mainly nitrophenols) in the cold period were tightly associated
485 with the impacts of old-age biomass material burning. These results were illustrated in



486 a diagram (**Figure 7**).

487 Biomass materials in rural China were typically old-age plant tissues, as
488 mentioned above. Fresh biomass materials (e.g., green vegetation) with the enrichment
489 of oils and proteins can exist in forest fires or wildfires. Indeed, previous studies have
490 suggested that biomass burning can lead to the formation of aerosol amines and nitriles.
491 However, no field observation studies have paid attention to the differences in aerosol
492 NOCs emitted from the combustion of fresh and old-age biomass materials. For the
493 first time, our results reveal that fresh biomass material combustion can contribute more
494 amines and nitriles than old-age biomass material combustion. Generally, this study
495 provides the field evidence on the differential impacts of combustion of fresh and old-
496 age biomass materials on aerosol NOCs, improving our current understanding of the
497 molecular compositions of organic nitrogen aerosols in a vast territory with a sparse
498 population in Northwest China. Moreover, according to the fact that the studied site is
499 highly affected by combustion emissions of different types of biomass materials, future
500 work is needed to deeply understand the quantitative contributions of different types of
501 biomass burning to OA in China.

502

503 **Data availability.** The data in this study are available at
504 <https://doi.org/10.5281/zenodo.10453929>

505

506 **Competing interests.** The authors declare no conflicts of interest relevant to this study.

507



508 **Supplement.** Details of chemical analysis and data processing, eight tables (Tables
509 S1–S8), and ten extensive figures (Figures S1–S10).

510

511 **Author contributions.** YX designed the study. YJM, TY, and HWX performed field
512 measurements and sample collection; YJM and TY performed chemical analysis; YX
513 and YJM performed data analysis; YX and YJM wrote the original manuscript; and YX,
514 YJM, HWX, and HYY reviewed and edited the manuscript.

515

516 **Financial support.** This study was kindly supported by the National Natural Science
517 Foundation of China through grant 42303081 (Y. Xu) and Shanghai “Science and
518 Technology Innovation Action Plan” Shanghai Sailing Program through grant
519 22YF1418700 (Y. Xu).

520

521 **References**

522 Aiken, A. C., Decarlo, P. F., Kroll, J. H., Worsnop, D. R., Huffman, J. A., Docherty,
523 K. S., Ulbrich, I. M., Mohr, C., Kimmel, J. R., Sueper, D., Sun, Y., Zhang, Q., Trimborn,
524 A., Northway, M., Ziemann, P. J., Canagaratna, M. R., Onasch, T. B., Alfarra, M. R.,
525 Prevot, A. S., Dommen, J., Duplissy, J., Metzger, A., Baltensperger, U., and Jimenez, J.
526 L.: O/C and OM/OC ratios of primary, secondary, and ambient organic aerosols with
527 high-resolution time-of-flight aerosol mass spectrometry, *Environ. Sci. Technol.*, 42,
528 4478–4485, <https://doi.org/10.1021/es703009q>, 2008.

529 Altieri, K. E., Fawcett, S. E., Peters, A. J., Sigman, D. M., and Hastings, M. G.:



- 530 Marine biogenic source of atmospheric organic nitrogen in the subtropical North
531 Atlantic, P. Natl. Acad. Sci. USA, 113, 925-930,
532 <https://doi.org/10.1073/pnas.1516847113>, 2016.
- 533 Bandowe, B. A. M. and Meusel, H.: Nitrated polycyclic aromatic hydrocarbons
534 (nitro-PAHs) in the environment – A review, Sci. Total Environ., 581-582, 237-257,
535 <https://doi.org/10.1016/j.scitotenv.2016.12.115>, 2017.
- 536 Bátori, Z., Erdős, L., Kelemen, A., Deák, B., Valkó, O., Gallé, R., Bragina, T. M.,
537 Kiss, P. J., Kröel-Dulay, G., and Tölgyesi, C.: Diversity patterns in sandy forest-steppes:
538 a comparative study from the western and central Palaearctic, Biodivers. Conserv., 27,
539 1011-1030, <https://doi.org/10.1007/s10531-017-1477-7>, 2018.
- 540 Cape, J. N., Cornell, S. E., Jickells, T. D., and Nemitz, E.: Organic nitrogen in the
541 atmosphere — Where does it come from? A review of sources and methods, Atmos.
542 Res., 102, 30-48, <https://doi.org/10.1016/j.atmosres.2011.07.009>, 2011.
- 543 Cecinato, A., Di Palo, V., Pomata, D., Tomasi Scianò, M. C., and Possanzini, M.:
544 Measurement of phase-distributed nitrophenols in Rome ambient air, Chemosphere, 59,
545 679-683, <https://doi.org/10.1016/j.chemosphere.2004.10.045>, 2005.
- 546 Chen, J., Li, C., Ristovski, Z., Milic, A., Gu, Y., Islam, M. S., Wang, S., Hao, J.,
547 Zhang, H., He, C., Guo, H., Fu, H., Miljevic, B., Morawska, L., Thai, P., Lam, Y. F.,
548 Pereira, G., Ding, A., Huang, X., and Dumka, U. C.: A review of biomass burning:
549 Emissions and impacts on air quality, health and climate in China, Sci. Total Environ.,
550 579, 1000-1034, <https://doi.org/10.1016/j.scitotenv.2016.11.025>, 2017.
- 551 De Haan, D. O., Hawkins, L. N., Welsh, H. G., Pednekar, R., Casar, J. R.,



- 552 Pennington, E. A., de Loera, A., Jimenez, N. G., Symons, M. A., Zauscher, M., Pajunoja,
553 A., Caponi, L., Cazaunau, M., Formenti, P., Gratien, A., Pangu, E., and Doussin, J.-F.:
554 Brown Carbon Production in Ammonium- or Amine-Containing Aerosol Particles by
555 Reactive Uptake of Methylglyoxal and Photolytic Cloud Cycling, *Environ. Sci.*
556 *Technol.*, 51, 7458-7466, <https://doi.org/10.1021/acs.est.7b00159>, 2017.
- 557 Ditto, J. C., Abbatt, J. P. D., and Chan, A. W. H.: Gas- and Particle-Phase Amide
558 Emissions from Cooking: Mechanisms and Air Quality Impacts, *Environ. Sci. Technol.*,
559 56, 7741-7750, <https://doi.org/10.1021/acs.est.2c01409>, 2022a.
- 560 Ditto, J. C., Machesky, J., and Gentner, D. R.: Analysis of reduced and oxidized
561 nitrogen-containing organic compounds at a coastal site in summer and winter, *Atmos.*
562 *Chem. Phys.*, 22, 3045-3065, <https://doi.org/10.5194/acp-22-3045-2022>, 2022b.
- 563 Ditto, J. C., Joo, T., Slade, J. H., Shepson, P. B., Ng, N. L., and Gentner, D. R.:
564 Nontargeted Tandem Mass Spectrometry Analysis Reveals Diversity and Variability in
565 Aerosol Functional Groups across Multiple Sites, Seasons, and Times of Day, *Environ.*
566 *Sci. Technol. Lett.*, 7, 60-69, <https://doi.org/10.1021/acs.estlett.9b00702>, 2020.
- 567 Dou, J., Lin, P., Kuang, B.-Y., and Yu, J. Z.: Reactive Oxygen Species Production
568 Mediated by Humic-like Substances in Atmospheric Aerosols: Enhancement Effects by
569 Pyridine, Imidazole, and Their Derivatives, *Environ. Sci. Technol.*, 49, 6457-6465,
570 <https://doi.org/10.1021/es5059378>, 2015.
- 571 Duan, J., Huang, R. J., Li, Y., Chen, Q., Zheng, Y., Chen, Y., Lin, C., Ni, H., Wang,
572 M., Ovadnevaite, J., Ceburnis, D., Chen, C., Worsnop, D. R., Hoffmann, T., O'Dowd,
573 C., and Cao, J.: Summertime and wintertime atmospheric processes of secondary



574 aerosol in Beijing, *Atmos. Chem. Phys.*, 20, 3793-3807, [https://doi.org/10.5194/acp-](https://doi.org/10.5194/acp-20-3793-2020)
575 [20-3793-2020](https://doi.org/10.5194/acp-20-3793-2020), 2020.

576 Ehhalt, D. H. and Rohrer, F.: Dependence of the OH concentration on solar UV, *J.*
577 *Geophys. Res.-Atmos.*, 105, 3565-3571, <https://doi.org/10.1029/1999JD901070>, 2000.

578 Franze, T., Weller, M. G., Niessner, R., and Pöschl, U.: Protein Nitration by
579 Polluted Air, *Environ. Sci. Technol.*, 39, 1673-1678, <https://doi.org/10.1021/es0488737>,
580 2005.

581 Frege, C., Ortega, I. K., Rissanen, M. P., Praplan, A. P., Steiner, G., Heinritzi, M.,
582 Ahonen, L., Amorim, A., Bernhammer, A. K., Bianchi, F., Brilke, S., Breitenlechner,
583 M., Dada, L., Dias, A., Duplissy, J., Ehrhart, S., El-Haddad, I., Fischer, L., Fuchs, C.,
584 Garmash, O., Gonin, M., Hansel, A., Hoyle, C. R., Jokinen, T., Junninen, H., Kirkby, J.,
585 Kürten, A., Lehtipalo, K., Leiminger, M., Mauldin, R. L., Molteni, U., Nichman, L.,
586 Petäjä, T., Sarnela, N., Schobesberger, S., Simon, M., Sipilä, M., Stolzenburg, D., Tomé,
587 A., Vogel, A. L., Wagner, A. C., Wagner, R., Xiao, M., Yan, C., Ye, P., Curtius, J.,
588 Donahue, N. M., Flagan, R. C., Kulmala, M., Worsnop, D. R., Winkler, P. M., Dommen,
589 J., and Baltensperger, U.: Influence of temperature on the molecular composition of
590 ions and charged clusters during pure biogenic nucleation, *Atmos. Chem. Phys.*, 18, 65-
591 79, <https://doi.org/10.5194/acp-18-65-2018>, 2018.

592 Guo, H., Xu, L., Bougiatioti, A., Cerully, K. M., Capps, S. L., Hite Jr, J. R., Carlton,
593 A. G., Lee, S. H., Bergin, M. H., Ng, N. L., Nenes, A., and Weber, R. J.: Fine-particle
594 water and pH in the southeastern United States, *Atmos. Chem. Phys.*, 15, 5211-5228,
595 <https://doi.org/10.5194/acp-15-5211-2015>, 2015.



- 596 Han, Y., Zhang, X., Li, L., Lin, Y., Zhu, C., Zhang, N., Wang, Q., and Cao, J.:
597 Enhanced Production of Organosulfur Species during a Severe Winter Haze Episode in
598 the Guanzhong Basin of Northwest China, *Environ. Sci. Technol.*,
599 <https://doi.org/10.1021/acs.est.3c02914>, 2023.
- 600 Harrison, M. A. J., Barra, S., Borghesi, D., Vione, D., Arsene, C., and Iulian Olariu,
601 R.: Nitrated phenols in the atmosphere: a review, *Atmos. Environ.*, 39, 231-248,
602 <https://doi.org/10.1016/j.atmosenv.2004.09.044>, 2005.
- 603 Iinuma, Y., Böge, O., Gräfe, R., and Herrmann, H.: Methyl-Nitrocatechols:
604 Atmospheric Tracer Compounds for Biomass Burning Secondary Organic Aerosols,
605 *Environ. Sci. Technol.*, 44, 8453-8459, <https://doi.org/10.1021/es102938a>, 2010.
- 606 Jian, Q., Boyer, T. H., Yang, X., Xia, B., and Yang, X.: Characteristics and DBP
607 formation of dissolved organic matter from leachates of fresh and aged leaf litter,
608 *Chemosphere*, 152, 335-344, <https://doi.org/10.1016/j.chemosphere.2016.02.107>, 2016.
- 609 Jiang, H., Li, J., Tang, J., Zhao, S., Chen, Y., Tian, C., Zhang, X., Jiang, B., Liao,
610 Y., and Zhang, G.: Factors Influencing the Molecular Compositions and Distributions
611 of Atmospheric Nitrogen-Containing Compounds, *J. Geophys. Res.-Atmos.*, 127,
612 e2021JD036284, <https://doi.org/10.1029/2021JD036284>, 2022.
- 613 Kenagy, H. S., Romer Present, P. S., Wooldridge, P. J., Nault, B. A., Campuzano-
614 Jost, P., Day, D. A., Jimenez, J. L., Zare, A., Pye, H. O. T., Yu, J., Song, C. H., Blake,
615 D. R., Woo, J.-H., Kim, Y., and Cohen, R. C.: Contribution of Organic Nitrates to
616 Organic Aerosol over South Korea during KORUS-AQ, *Environ. Sci. Technol.*, 55,
617 16326-16338, <https://doi.org/10.1021/acs.est.1c05521>, 2021.



618 Koch, B. P. and Dittmar, T.: From mass to structure: an aromaticity index for high-
619 resolution mass data of natural organic matter, *Rapid Commun. Mass Spectrom.*, 20,
620 926-932, <https://doi.org/10.1002/rem.2386>, 2006.

621 Kondo, Y., Miyazaki, Y., Takegawa, N., Miyakawa, T., Weber, R. J., Jimenez, J.
622 L., Zhang, Q., and Worsnop, D. R.: Oxygenated and water-soluble organic aerosols in
623 Tokyo, *J. Geophys. Res.-Atmos.*, 112, <https://doi.org/10.1029/2006JD007056>, 2007.

624 Kourtchev, I., Godoi, R. H. M., Connors, S., Levine, J. G., Archibald, A. T., Godoi,
625 A. F. L., Paralovo, S. L., Barbosa, C. G. G., Souza, R. A. F., Manzi, A. O., Seco, R.,
626 Sjostedt, S., Park, J. H., Guenther, A., Kim, S., Smith, J., Martin, S. T., and Kalberer,
627 M.: Molecular composition of organic aerosols in central Amazonia: an ultra-high-
628 resolution mass spectrometry study, *Atmos. Chem. Phys.*, 16, 11899-11913,
629 <https://doi.org/10.5194/acp-16-11899-2016>, 2016.

630 Kroll, J. H., Donahue, N. M., Jimenez, J. L., Kessler, S. H., Canagaratna, M. R.,
631 Wilson, K. R., Altieri, K. E., Mazzoleni, L. R., Wozniak, A. S., Bluhm, H., Mysak, E.
632 R., Smith, J. D., Kolb, C. E., and Worsnop, D. R.: Carbon oxidation state as a metric
633 for describing the chemistry of atmospheric organic aerosol, *Nat. Chem.*, 3, 133-139,
634 <https://doi.org/10.1038/nchem.948>, 2011.

635 Laskin, A., Smith, J. S., and Laskin, J.: Molecular Characterization of Nitrogen-
636 Containing Organic Compounds in Biomass Burning Aerosols Using High-Resolution
637 Mass Spectrometry, *Environ. Sci. Technol.*, 43, 3764-3771,
638 <https://doi.org/10.1021/es803456n>, 2009.

639 Laskin, J., Laskin, A., Nizkorodov, S. A., Roach, P., Eckert, P., Gilles, M. K., Wang,



640 B., Lee, H. J., and Hu, Q.: Molecular Selectivity of Brown Carbon Chromophores,
641 Environ. Sci. Technol., 48, 12047-12055, <https://doi.org/10.1021/es503432r>, 2014.

642 Lee, B. H., Mohr, C., Lopez-Hilfiker, F. D., Lutz, A., Hallquist, M., Lee, L., Romer,
643 P., Cohen, R. C., Iyer, S., Kurtén, T., Hu, W., Day, D. A., Campuzano-Jost, P., Jimenez,
644 J. L., Xu, L., Ng, N. L., Guo, H., Weber, R. J., Wild, R. J., Brown, S. S., Koss, A., de
645 Gouw, J., Olson, K., Goldstein, A. H., Seco, R., Kim, S., McAvey, K., Shepson, P. B.,
646 Starn, T., Baumann, K., Edgerton, E. S., Liu, J., Shilling, J. E., Miller, D. O., Brune, W.,
647 Schobesberger, S., D'Ambro, E. L., and Thornton, J. A.: Highly functionalized organic
648 nitrates in the southeast United States: Contribution to secondary organic aerosol and
649 reactive nitrogen budgets, P. Natl. Acad. Sci. USA, 113, 1516-1521,
650 <https://doi.org/10.1073/pnas.1508108113>, 2016.

651 Li, S., Liu, D., Kong, S., Wu, Y., Hu, K., Zheng, H., Cheng, Y., Zheng, S., Jiang,
652 X., Ding, S., Hu, D., Liu, Q., Tian, P., Zhao, D., and Sheng, J.: Evolution of source
653 attributed organic aerosols and gases in a megacity of central China, Atmos. Chem.
654 Phys., 22, 6937-6951, <https://doi.org/10.5194/acp-22-6937-2022>, 2022.

655 Li, Y., Chen, M., Wang, Y., Huang, T., Wang, G., Li, Z., Li, J., Meng, J., and Hou,
656 Z.: Seasonal characteristics and provenance of organic aerosols in the urban atmosphere
657 of Liaocheng in the North China Plain: Significant effect of biomass burning,
658 Particuology, 75, 185-198, <https://doi.org/10.1016/j.partic.2022.07.012>, 2023.

659 Lin, P., Rincon, A. G., Kalberer, M., and Yu, J. Z.: Elemental Composition of
660 HULIS in the Pearl River Delta Region, China: Results Inferred from Positive and
661 Negative Electrospray High Resolution Mass Spectrometric Data, Environ. Sci.



662 Technol., 46, 7454-7462, <https://doi.org/10.1021/es300285d>, 2012.

663 Lin, X., Xu, Y., Zhu, R.-G., Xiao, H.-W., and Xiao, H.-Y.: Proteinaceous Matter in
664 PM_{2.5} in Suburban Guiyang, Southwestern China: Decreased Importance in Long-
665 Range Transport and Atmospheric Degradation, *J. Geophys. Res.-Atmos.*, 128,
666 e2023JD038516, <https://doi.org/10.1029/2023JD038516>, 2023.

667 Liu, T., Xu, Y., Sun, Q.-B., Xiao, H.-W., Zhu, R.-G., Li, C.-X., Li, Z.-Y., Zhang,
668 K.-Q., Sun, C.-X., and Xiao, H.-Y.: Characteristics, Origins, and Atmospheric
669 Processes of Amines in Fine Aerosol Particles in Winter in China, *J. Geophys. Res.-*
670 *Atmos.*, 128, e2023JD038974, <https://doi.org/10.1029/2023JD038974>, 2023.

671 Liu, T., Hong, Y., Li, M., Xu, L., Chen, J., Bian, Y., Yang, C., Dan, Y., Zhang, Y.,
672 Xue, L., Zhao, M., Huang, Z., and Wang, H.: Atmospheric oxidation capacity and ozone
673 pollution mechanism in a coastal city of southeastern China: analysis of a typical
674 photochemical episode by an observation-based model, *Atmos. Chem. Phys.*, 22, 2173-
675 2190, <https://doi.org/10.5194/acp-22-2173-2022>, 2022.

676 Ma, L., Guzman, C., Niedeck, C., Tran, T., Zhang, Q., and Anastasio, C.: Kinetics
677 and Mass Yields of Aqueous Secondary Organic Aerosol from Highly Substituted
678 Phenols Reacting with a Triplet Excited State, *Environ. Sci. Technol.*, 55, 5772-5781,
679 <https://doi.org/10.1021/acs.est.1c00575>, 2021.

680 Miyazaki, Y., Fu, P., Ono, K., Tachibana, E., and Kawamura, K.: Seasonal cycles
681 of water-soluble organic nitrogen aerosols in a deciduous broadleaf forest in northern
682 Japan, *J. Geophys. Res.-Atmos.*, 119, 1440-1454,
683 <https://doi.org/10.1002/2013JD020713>, 2014.



684 Nguyen, T. B., Bates, K. H., Crounse, J. D., Schwantes, R. H., Zhang, X.,
685 Kjaergaard, H. G., Surratt, J. D., Lin, P., Laskin, A., Seinfeld, J. H., and Wennberg, P.
686 O.: Mechanism of the hydroxyl radical oxidation of methacryloyl peroxyxynitrate (MPAN)
687 and its pathway toward secondary organic aerosol formation in the atmosphere, *Phys.*
688 *Chem. Chem. Phys.*, 17, 17914-17926, <https://doi.org/10.1039/C5CP02001H>, 2015.

689 Perring, A. E., Pusede, S. E., and Cohen, R. C.: An Observational Perspective on
690 the Atmospheric Impacts of Alkyl and Multifunctional Nitrates on Ozone and
691 Secondary Organic Aerosol, *Chem. Rev.*, 113, 5848-5870,
692 <https://doi.org/10.1021/cr300520x>, 2013.

693 Qiu, C. and Zhang, R.: Multiphase chemistry of atmospheric amines, *Phys. Chem.*
694 *Chem. Phys.*, 15, 5738-5752, <https://doi.org/10.1039/C3CP43446j>, 2013.

695 Qizhi, M., Ying, L., Kang, W., and Qingfei, Z.: Spatio-Temporal Changes of
696 Population Density and Urbanization Pattern in China(2000–2010), *China City Plan.*
697 *Rev.*, 25, 8-14, 2016.

698 Radzi Bin Abas, M., Rahman, N. A., Omar, N. Y. M. J., Maah, M. J., Abu Samah,
699 A., Oros, D. R., Otto, A., and Simoneit, B. R. T.: Organic composition of aerosol
700 particulate matter during a haze episode in Kuala Lumpur, Malaysia, *Atmos. Environ.*,
701 38, 4223-4241, <https://doi.org/10.1016/j.atmosenv.2004.01.048>, 2004.

702 Ren, Y., Wang, G., Wu, C., Wang, J., Li, J., Zhang, L., Han, Y., Liu, L., Cao, C.,
703 Cao, J., He, Q., and Liu, X.: Changes in concentration, composition and source
704 contribution of atmospheric organic aerosols by shifting coal to natural gas in Urumqi,
705 *Atmos. Environ.*, 148, 306-315, <https://doi.org/10.1016/j.atmosenv.2016.10.053>, 2017.



706 Rollins, A. W., Browne, E. C., Min, K.-E., Pusede, S. E., Wooldridge, P. J., Gentner,
707 D. R., Goldstein, A. H., Liu, S., Day, D. A., Russell, L. M., and Cohen, R. C.: Evidence
708 for NO_x Control over Nighttime SOA Formation, *Science*, 337, 1210-1212,
709 <https://doi.org/10.1126/science.1221520>, 2012.

710 Salvador, C. M. G., Tang, R., Priestley, M., Li, L., Tsiligiannis, E., Le Breton, M.,
711 Zhu, W., Zeng, L., Wang, H., Yu, Y., Hu, M., Guo, S., and Hallquist, M.: Ambient nitro-
712 aromatic compounds – biomass burning versus secondary formation in rural China,
713 *Atmos. Chem. Phys.*, 21, 1389-1406, <https://doi.org/10.5194/acp-21-1389-2021>, 2021.

714 Samy, S. and Hays, M. D.: Quantitative LC–MS for water-soluble heterocyclic
715 amines in fine aerosols (PM_{2.5}) at Duke Forest, USA, *Atmos. Environ.*, 72, 77-80,
716 <https://doi.org/10.1016/j.atmosenv.2013.02.032>, 2013.

717 Schauer, J. J., Kleeman, M. J., Cass, G. R., and Simoneit, B. R. T.: Measurement
718 of Emissions from Air Pollution Sources. 1. C₁ through C₂₉ Organic Compounds from
719 Meat Charbroiling, *Environ. Sci. Technol.*, 33, 1566-1577,
720 <https://doi.org/10.1021/es980076j>, 1999.

721 Seinfeld, J. H., Bretherton, C., Carslaw, K. S., Coe, H., DeMott, P. J., Dunlea, E.
722 J., Feingold, G., Ghan, S., Guenther, A. B., Kahn, R., Kraucunas, I., Kreidenweis, S.
723 M., Molina, M. J., Nenes, A., Penner, J. E., Prather, K. A., Ramanathan, V., Ramaswamy,
724 V., Rasch, P. J., Ravishankara, A. R., Rosenfeld, D., Stephens, G., and Wood, R.:
725 Improving our fundamental understanding of the role of aerosol–cloud interactions in
726 the climate system, *P. Natl. Acad. Sci. USA*, 113, 5781-5790,
727 <https://doi.org/10.1073/pnas.1514043113>, 2016.



728 Simoneit, B. R. T., Rushdi, A. I., bin Abas, M. R., and Didyk, B. M.: Alkyl Amides
729 and Nitriles as Novel Tracers for Biomass Burning, *Environ. Sci. Technol.*, 37, 16-21,
730 <https://doi.org/10.1021/es020811y>, 2003.

731 Smith, J. D., Sio, V., Yu, L., Zhang, Q., and Anastasio, C.: Secondary Organic
732 Aerosol Production from Aqueous Reactions of Atmospheric Phenols with an Organic
733 Triplet Excited State, *Environ. Sci. Technol.*, 48, 1049-1057,
734 <https://doi.org/10.1021/es4045715>, 2014.

735 Song, J., Li, M., Jiang, B., Wei, S., Fan, X., and Peng, P. a.: Molecular
736 Characterization of Water-Soluble Humic like Substances in Smoke Particles Emitted
737 from Combustion of Biomass Materials and Coal Using Ultrahigh-Resolution
738 Electrospray Ionization Fourier Transform Ion Cyclotron Resonance Mass
739 Spectrometry, *Environ. Sci. Technol.*, 52, 2575-2585,
740 <https://doi.org/10.1021/acs.est.7b06126>, 2018.

741 Song, J., Li, M., Zou, C., Cao, T., Fan, X., Jiang, B., Yu, Z., Jia, W., and Peng, P.
742 a.: Molecular Characterization of Nitrogen-Containing Compounds in Humic-like
743 Substances Emitted from Biomass Burning and Coal Combustion, *Environ. Sci.*
744 *Technol.*, 56, 119-130, <https://doi.org/10.1021/acs.est.1c04451>, 2022.

745 Stolzenburg, D., Fischer, L., Vogel, A. L., Heinritzi, M., Schervish, M., Simon, M.,
746 Wagner, A. C., Dada, L., Ahonen, L. R., Amorim, A., Baccarini, A., Bauer, P. S.,
747 Baumgartner, B., Bergen, A., Bianchi, F., Breitenlechner, M., Brilke, S., Buenrostro
748 Mazon, S., Chen, D., Dias, A., Draper, D. C., Duplissy, J., El Haddad, I., Finkenzeller,
749 H., Frege, C., Fuchs, C., Garmash, O., Gordon, H., He, X., Helm, J., Hofbauer, V.,



750 Hoyle, C. R., Kim, C., Kirkby, J., Kontkanen, J., Kürten, A., Lampilahti, J., Lawler, M.,
751 Lehtipalo, K., Leiminger, M., Mai, H., Mathot, S., Mentler, B., Molteni, U., Nie, W.,
752 Nieminen, T., Nowak, J. B., Ojdanic, A., Onnela, A., Passananti, M., Petäjä, T.,
753 Quéléver, L. L. J., Rissanen, M. P., Sarnela, N., Schallhart, S., Tauber, C., Tomé, A.,
754 Wagner, R., Wang, M., Weitz, L., Wimmer, D., Xiao, M., Yan, C., Ye, P., Zha, Q.,
755 Baltensperger, U., Curtius, J., Dommen, J., Flagan, R. C., Kulmala, M., Smith, J. N.,
756 Worsnop, D. R., Hansel, A., Donahue, N. M., and Winkler, P. M.: Rapid growth of
757 organic aerosol nanoparticles over a wide tropospheric temperature range, *P. Natl. Acad.*
758 *Sci. USA*, 115, 9122-9127, <https://doi.org/10.1073/pnas.1807604115>, 2018.

759 Surratt, J. D., Chan, A. W. H., Eddingsaas, N. C., Chan, M., Loza, C. L., Kwan, A.
760 J., Hersey, S. P., Flagan, R. C., Wennberg, P. O., and Seinfeld, J. H.: Reactive
761 intermediates revealed in secondary organic aerosol formation from isoprene, *P. Natl.*
762 *Acad. Sci. USA*, 107, 6640-6645, <https://doi.org/10.1073/pnas.0911114107>, 2010.

763 Tomsche, L., Piel, F., Mikoviny, T., Nielsen, C. J., Guo, H., Campuzano-Jost, P.,
764 Nault, B. A., Schueneman, M. K., Jimenez, J. L., Halliday, H., Diskin, G., DiGangi, J.
765 P., Nowak, J. B., Wiggins, E. B., Gargulinski, E., Soja, A. J., and Wisthaler, A.:
766 Measurement report: Emission factors of NH₃ and NH_x for wildfires and agricultural
767 fires in the United States, *Atmos. Chem. Phys.*, 23, 2331-2343,
768 <https://doi.org/10.5194/acp-23-2331-2023>, 2023.

769 W. Hogg, R. and T. Gillan, F.: Fatty acids, sterols and hydrocarbons in the leaves
770 from eleven species of mangrove, *Phytochemistry*, 23, 93-97,
771 [https://doi.org/10.1016/0031-9422\(84\)83084-8](https://doi.org/10.1016/0031-9422(84)83084-8), 1984.



772 Wan, X., Qin, F., Cui, F., Chen, W., Ding, H., and Li, C.: Correlation between the
773 distribution of solar energy resources and the cloud cover in Xinjiang, IOP Conf. Ser.:
774 Earth Environ. Sci., 675, 012060, <https://doi.org/10.1088/1755-1315/675/1/012060>,
775 2021.

776 Wang, H., Wang, Q., Gao, Y., Zhou, M., Jing, S., Qiao, L., Yuan, B., Huang, D.,
777 Huang, C., Lou, S., Yan, R., de Gouw, J. A., Zhang, X., Chen, J., Chen, C., Tao, S., An,
778 J., and Li, Y.: Estimation of Secondary Organic Aerosol Formation During a
779 Photochemical Smog Episode in Shanghai, China, J. Geophys. Res.-Atmos., 125,
780 e2019JD032033, <https://doi.org/10.1029/2019JD032033>, 2020.

781 Wang, K., Huang, R.-J., Brüeggemann, M., Zhang, Y., Yang, L., Ni, H., Guo, J.,
782 Wang, M., Han, J., Bilde, M., Glasius, M., and Hoffmann, T.: Urban organic aerosol
783 composition in eastern China differs from north to south: molecular insight from a
784 liquid chromatography-mass spectrometry (Orbitrap) study, Atmos. Chem. Phys., 21,
785 9089-9104, <https://doi.org/10.5194/acp-21-9089-2021>, 2021a.

786 Wang, L., Zhang, K., Huang, W., Han, W., and Tian, C.-Y.: Seed oil content and
787 fatty acid composition of annual halophyte Suaeda acuminata: A comparative study on
788 dimorphic seeds, Afr. J. Biotechnol., 10, 19106-19108,
789 <https://doi.org/10.5897/ajb11.2597>, 2011.

790 Wang, Q., Shao, M., Zhang, Y., Wei, Y., Hu, M., and Guo, S.: Source
791 apportionment of fine organic aerosols in Beijing, Atmos. Chem. Phys., 9, 8573-8585,
792 <https://doi.org/10.5194/acp-9-8573-2009>, 2009.

793 Wang, X., Hayeck, N., Brüggemann, M., Yao, L., Chen, H., Zhang, C., Emmelin,



794 C., Chen, J., George, C., and Wang, L.: Chemical Characteristics of Organic Aerosols
795 in Shanghai: A Study by Ultrahigh-Performance Liquid Chromatography Coupled With
796 Orbitrap Mass Spectrometry, *J. Geophys. Res.-Atmos.*, 122, 11,703-711,722,
797 <https://doi.org/10.1002/2017JD026930>, 2017a.

798 Wang, X., Shen, Z., Liu, F., Lu, D., Tao, J., Lei, Y., Zhang, Q., Zeng, Y., Xu, H.,
799 Wu, Y., Zhang, R., and Cao, J.: Saccharides in summer and winter PM_{2.5} over Xi'an,
800 Northwestern China: Sources, and yearly variations of biomass burning contribution to
801 PM_{2.5}, *Atmos. Res.*, 214, 410-417, <https://doi.org/10.1016/j.atmosres.2018.08.024>,
802 2018.

803 Wang, Y., Zhao, Y., Li, Z., Li, C., Yan, N., and Xiao, H.: Importance of Hydroxyl
804 Radical Chemistry in Isoprene Suppression of Particle Formation from α -Pinene
805 Ozonolysis, *ACS Earth Space Chem.*, 5, 487-499,
806 <https://doi.org/10.1021/acsearthspacechem.0c00294>, 2021b.

807 Wang, Y., Hu, M., Lin, P., Guo, Q., Wu, Z., Li, M., Zeng, L., Song, Y., Zeng, L.,
808 Wu, Y., Guo, S., Huang, X., and He, L.: Molecular Characterization of Nitrogen-
809 Containing Organic Compounds in Humic-like Substances Emitted from Straw
810 Residue Burning, *Environ. Sci. Technol.*, 51, 5951-5961,
811 <https://doi.org/10.1021/acs.est.7b00248>, 2017b.

812 Wang, Y., Hu, M., Hu, W., Zheng, J., Niu, H., Fang, X., Xu, N., Wu, Z., Guo, S.,
813 Wu, Y., Chen, W., Lu, S., Shao, M., Xie, S., Luo, B., and Zhang, Y.: Secondary
814 Formation of Aerosols Under Typical High-Humidity Conditions in Wintertime
815 Sichuan Basin, China: A Contrast to the North China Plain, *J. Geophys. Res.-Atmos.*,



816 126, e2021JD034560, <https://doi.org/10.1029/2021JD034560>, 2021c.

817 Xie, Q., Su, S., Chen, S., Xu, Y., Cao, D., Chen, J., Ren, L., Yue, S., Zhao, W., Sun,
818 Y., Wang, Z., Tong, H., Su, H., Cheng, Y., Kawamura, K., Jiang, G., Liu, C. Q., and Fu,
819 P.: Molecular characterization of firework-related urban aerosols using Fourier
820 transform ion cyclotron resonance mass spectrometry, *Atmos. Chem. Phys.*, 20, 6803-
821 6820, <https://doi.org/10.5194/acp-20-6803-2020>, 2020.

822 Xu, Y. and Xiao, H.: Concentrations and nitrogen isotope compositions of free
823 amino acids in *Pinus massoniana* (Lamb.) needles of different ages as indicators of
824 atmospheric nitrogen pollution, *Atmos. Environ.*, 164, 348-359,
825 <https://doi.org/10.1016/j.atmosenv.2017.06.024>, 2017.

826 Xu, Y., Lin, Z., and Wu, C.: Spatiotemporal Variation of the Burned Area and Its
827 Relationship with Climatic Factors in Central Kazakhstan, *Remote Sens.*, 13, 313,
828 <https://doi.org/10.3390/rs13020313>, 2021.

829 Xu, Y., Dong, X.-N., Xiao, H.-Y., He, C., and Wu, D.-S.: Water-Insoluble
830 Components in Rainwater in Suburban Guiyang, Southwestern China: A Potential
831 Contributor to Dissolved Organic Carbon, *J. Geophys. Res.-Atmos.*, 127,
832 e2022JD037721, <https://doi.org/10.1029/2022JD037721>, 2022a.

833 Xu, Y., Dong, X.-N., Xiao, H.-Y., Zhou, J.-X., and Wu, D.-S.: Proteinaceous
834 Matter and Liquid Water in Fine Aerosols in Nanchang, Eastern China: Seasonal
835 Variations, Sources, and Potential Connections, *J. Geophys. Res.-Atmos.*, 127,
836 e2022JD036589, <https://doi.org/10.1029/2022JD036589>, 2022b.

837 Xu, Y., Dong, X. N., He, C., Wu, D. S., Xiao, H. W., and Xiao, H. Y.: Mist cannon



838 trucks can exacerbate the formation of water-soluble organic aerosol and PM_{2.5}
839 pollution in the road environment, *Atmos. Chem. Phys.*, *23*, 6775-6788,
840 <https://doi.org/10.5194/acp-23-6775-2023>, 2023.

841 Xu, Y., Miyazaki, Y., Tachibana, E., Sato, K., Ramasamy, S., Mochizuki, T.,
842 Sadanaga, Y., Nakashima, Y., Sakamoto, Y., Matsuda, K., and Kajii, Y.: Aerosol Liquid
843 Water Promotes the Formation of Water-Soluble Organic Nitrogen in Submicrometer
844 Aerosols in a Suburban Forest, *Environ. Sci. Technol.*, *54*, 1406-1414,
845 <https://dx.doi.org/10.1021/acs.est.9b05849>, 2020.

846 Yang, T., Xu, Y., Ye, Q., Ma, Y. J., Wang, Y. C., Yu, J. Z., Duan, Y. S., Li, C. X.,
847 Xiao, H. W., Li, Z. Y., Zhao, Y., and Xiao, H. Y.: Spatial and diurnal variations of aerosol
848 organosulfates in summertime Shanghai, China: potential influence of photochemical
849 processes and anthropogenic sulfate pollution, *Atmos. Chem. Phys.*, *23*, 13433-13450,
850 <https://doi.org/10.5194/acp-23-13433-2023>, 2023.

851 Zahardis, J., Geddes, S., and Petrucci, G. A.: The ozonolysis of primary aliphatic
852 amines in fine particles, *Atmos. Chem. Phys.*, *8*, 1181-1194,
853 <https://doi.org/10.5194/acp-8-1181-2008>, 2008.

854 Zarzana, K. J., De Haan, D. O., Freedman, M. A., Hasenkopf, C. A., and Tolbert,
855 M. A.: Optical Properties of the Products of α -Dicarbonyl and Amine Reactions in
856 Simulated Cloud Droplets, *Environ. Sci. Technol.*, *46*, 4845-4851,
857 <https://doi.org/10.1021/es2040152>, 2012.

858 Zhang, Q., Jimenez, J. L., Canagaratna, M. R., Allan, J. D., Coe, H., Ulbrich, I.,
859 Alfarra, M. R., Takami, A., Middlebrook, A. M., Sun, Y. L., Dzepina, K., Dunlea, E.,



860 Docherty, K., DeCarlo, P. F., Salcedo, D., Onasch, T., Jayne, J. T., Miyoshi, T., Shimono,
861 A., Hatakeyama, S., Takegawa, N., Kondo, Y., Schneider, J., Drewnick, F., Borrmann,
862 S., Weimer, S., Demerjian, K., Williams, P., Bower, K., Bahreini, R., Cottrell, L., Griffin,
863 R. J., Rautiainen, J., Sun, J. Y., Zhang, Y. M., and Worsnop, D. R.: Ubiquity and
864 dominance of oxygenated species in organic aerosols in anthropogenically-influenced
865 Northern Hemisphere midlatitudes, *Geophys. Res. Lett.*, 34,
866 <https://doi.org/10.1029/2007GL029979>, 2007.

867 Zhao, Y., Hu, M., Slanina, S., and Zhang, Y.: Chemical Compositions of Fine
868 Particulate Organic Matter Emitted from Chinese Cooking, *Environ. Sci. Technol.*, 41,
869 99-105, <https://doi.org/10.1021/es0614518>, 2007.

870 Zhong, S., Chen, S., Deng, J., Fan, Y., Zhang, Q., Xie, Q., Qi, Y., Hu, W., Wu, L.,
871 Li, X., Pavuluri, C. M., Zhu, J., Wang, X., Liu, D., Pan, X., Sun, Y., Wang, Z., Xu, Y.,
872 Tong, H., Su, H., Cheng, Y., Kawamura, K., and Fu, P.: Impact of biogenic secondary
873 organic aerosol (SOA) loading on the molecular composition of wintertime PM_{2.5} in
874 urban Tianjin: an insight from Fourier transform ion cyclotron resonance mass
875 spectrometry, *Atmos. Chem. Phys.*, 23, 2061-2077, [https://doi.org/10.5194/acp-23-](https://doi.org/10.5194/acp-23-2061-2023)
876 [2061-2023](https://doi.org/10.5194/acp-23-2061-2023), 2023.

877 Zhou, S., Guo, F., Chao, C.-Y., Yoon, S., Alvarez, S. L., Shrestha, S., Flynn, J. H.,
878 III, Usenko, S., Sheesley, R. J., and Griffin, R. J.: Marine Submicron Aerosols from the
879 Gulf of Mexico: Polluted and Acidic with Rapid Production of Sulfate and
880 Organosulfates, *Environ. Sci. Technol.*, 57, 5149-5159,
881 <https://doi.org/10.1021/acs.est.2c05469>, 2023.

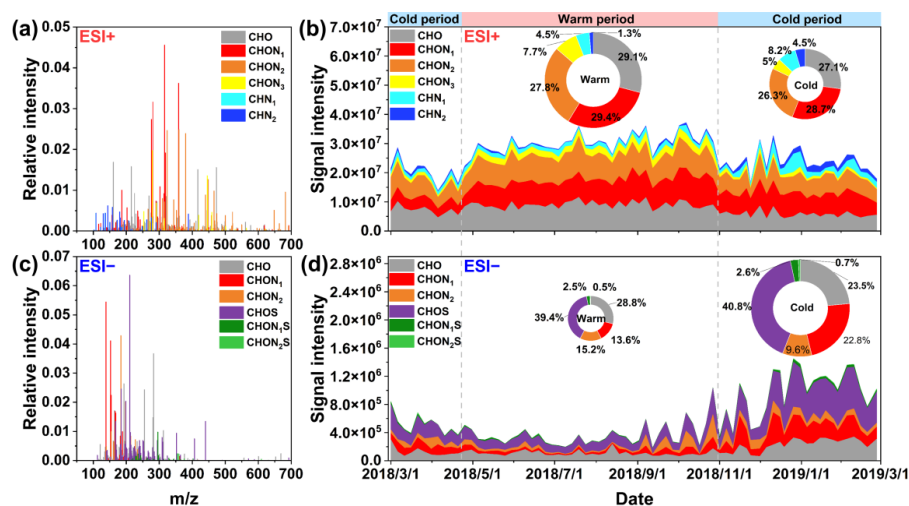


882 Zou, C., Cao, T., Li, M., Song, J., Jiang, B., Jia, W., Li, J., Ding, X., Yu, Z., Zhang,
883 G., and Peng, P.: Measurement report: Changes in light absorption and molecular
884 composition of water-soluble humic-like substances during a winter haze bloom-decay
885 process in Guangzhou, China, Atmos. Chem. Phys., 23, 963-979,
886 <https://doi.org/10.5194/acp-23-963-2023>, 2023.

887



888 **Figure 1.**



889

890 **Figure 1.** The reconstructed mass spectrum distribution of the detected species in PM_{2.5}

891 in (a) ESI+ and (c) ESI- modes during the whole campaign. Temporal variations in the

892 fractional distribution of classified compounds in (b) ESI+ and (d) ESI- modes. The

893 ring diagrams inside the panel show the signal intensity fractions of classified

894 compounds, the size of which is proportional to the total signal intensity of all species

895 detected in PM_{2.5} in different periods.

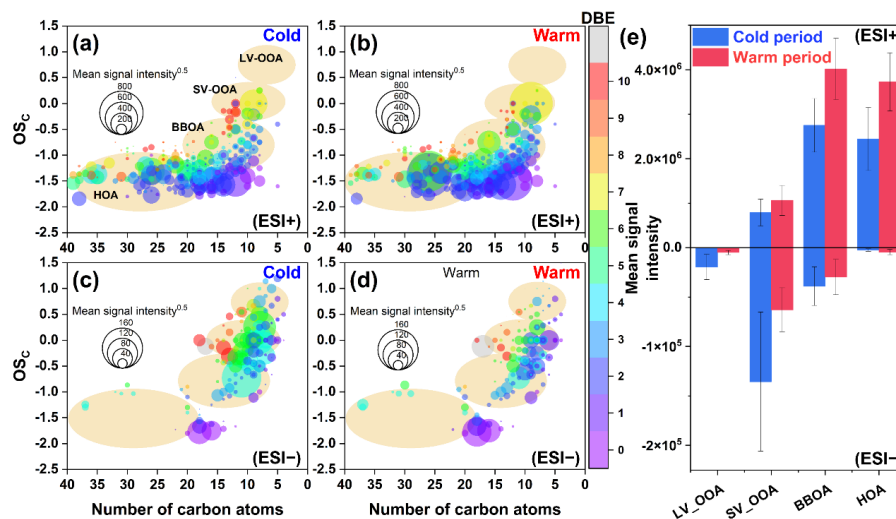
896

897

898



899 **Figure 2.**



900

901 **Figure 2.** OSc values of CHO molecules detected in (a and b) ESI+ and (c and d) ESI-

902 modes in PM_{2.5} collected from different periods (cold vs. warm). The size and color of

903 the circle indicate the mean signal intensity and DBE value of compounds, respectively.

904 The light-orange background indicates the areas of low-volatility oxidized OA (LV-

905 OOA), semivolatile oxidized OA (SV-OOA), biomass burning-like OA (BBOA), and

906 hydrocarbon-like OA (HOA) (Kroll et al., 2011), according to which (e) the mean signal

907 intensity of classified compounds was calculated for samples from different periods.

908

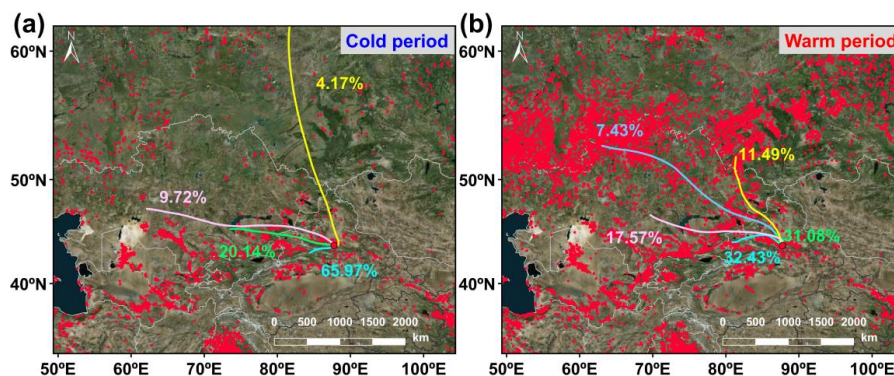
909

910

911



912 **Figure 3**



913

914 **Figure 3.** The 3-day (72 h) back trajectories illustrating the typical air mass flows to

915 the study site during the (a) warm and (b) cool periods. Fire spots were shown in red,

916 which was created based on NASA active fire data (VIIRS 375 m,

917 https://firms.modaps.eosdis.nasa.gov/active_fire/). The map was derived from

918 ©MeteoInfoMap (version 3.6.2) (Chinese Academy of Meteorological Sciences, China).

919

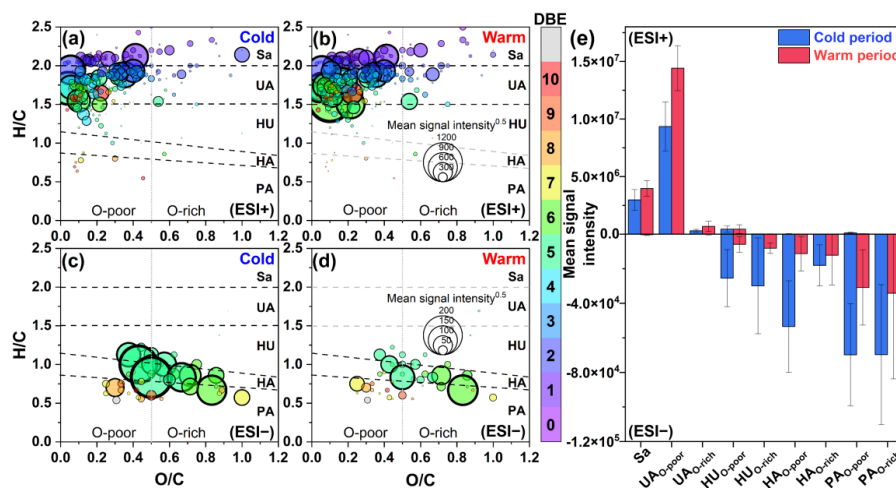
920

921

922



923 **Figure 4.**



924

925 **Figure 4.** Van Krevelen diagrams of CHON molecules detected in (a and b) ESI+ and
926 (c and d) ESI- modes in PM_{2.5} collected from different periods (cold vs. warm). The
927 subgroups in the panel include saturated-like (Sa), unsaturated aliphatic-like (UA),
928 highly unsaturated-like (HU), highly aromatic-like (HA), and polycyclic aromatic-like
929 (PA) compounds, further distinguishing between oxygen-poor and oxygen-rich
930 compounds with an oxygen to carbon ratio of 0.5. The size and color of the circle
931 indicate the mean signal intensity and DBE value of compounds, respectively. The (e)
932 mean signal intensity of classified compounds was calculated for samples from
933 different periods.

934

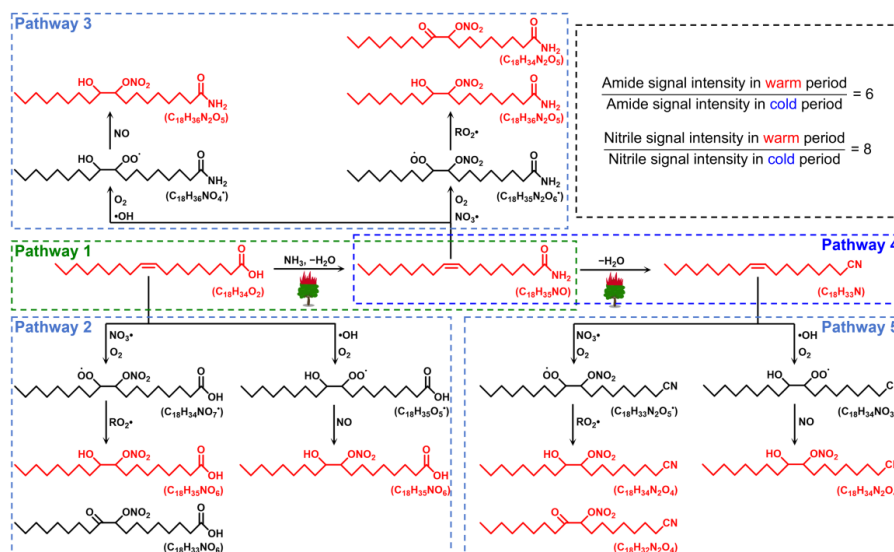
935

936

937



938 **Figure 5.**



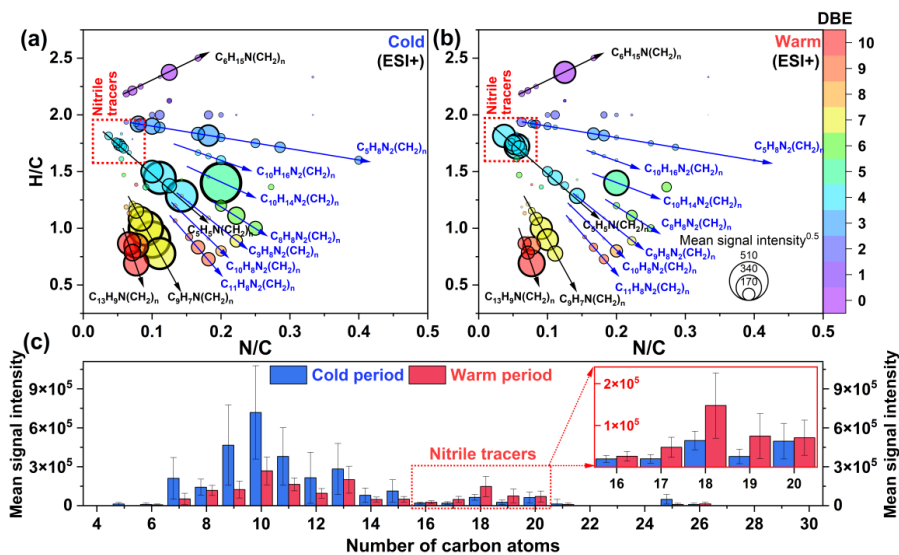
939

940 **Figure 5.** Proposed pathways for the reaction of carboxylic acids (oleic acid as a
 941 representative) with ammonia to form the observed NOCs in $PM_{2.5}$ under the influence
 942 of the high temperature generated during wildfires or forest fires. Compounds observed
 943 in $PM_{2.5}$ were shown in red.

944



945 **Figure 6.**



946

947 **Figure 6.** Van Krevelen diagrams of CHN molecules detected in PM_{2.5} collected from

948 the (a) cold and (b) warm periods. The size and color of the circle indicate the mean

949 signal intensity and DBE value of compounds, respectively. The mean signal intensity

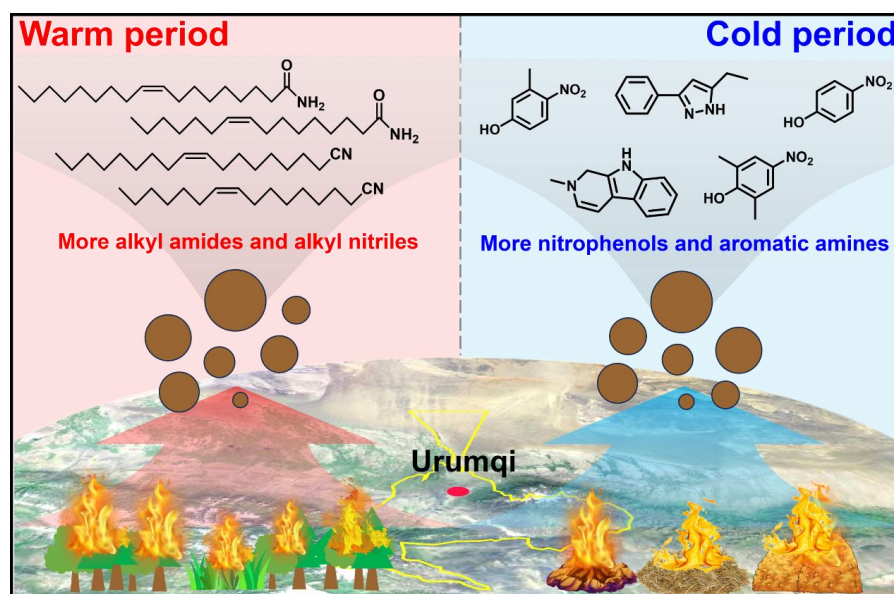
950 distributions of (c) carbon atoms in CHN molecules detected in PM_{2.5} collected from

951 the cold and warm periods

952



953 **Figure 7.**



954

955 **Figure 7.** Conceptual picture showing the differential impacts of combustion of fresh

956 and old-age biomass materials on aerosol NOCs in suburban Urumqi. The map was

957 derived from ©Baidu Maps (BIDU, China).